

Equidistant Spectral Lines in Train Vibrations

by Florian Fuchs, Götz Bokelmann, and the AlpArray Working Group

ABSTRACT

We analyze in detail the seismic vibrations generated by trains, measured at distance from the track with high sensitivity broadband sensors installed for the AlpArray project. The geometrical restrictions of the network resulted in a number of instruments deployed in the vicinity of railway lines. On seismic stations within 1.5 km of a railway, we observe characteristic seismic signals that we can relate to the passage of trains. All train signals share a characteristic feature of sharp equidistant spectral lines in the entire 2–40 Hz frequency range. For a site located 300 m from a busy track, frequency spacing is between 1 and 2 Hz and relates to train speed. The spectrograms of individual trains show acceleration and deceleration phases that match well with the expected driving profile for different types of trains. We discuss possible mechanisms responsible for the strikingly equidistant spectral lines. We search for Doppler effects and compare the observations with theoretically expected values. Based on cepstrum analysis, we suggest quasi-static axle load by consecutive bogies as the dominant mechanism behind the 1–2 Hz line spacing. The striking feature of the equidistant spectral lines within the train vibrations renders them outstanding seismic sources which may have potential for seismic imaging and attenuation studies.

Electronic Supplement: Figures showing the seismic station distribution and examples of Doppler effect visible in the spectrograms.

INTRODUCTION

Train-induced vibrations are mainly regarded as a source of unwanted noise for classical seismological applications such as earthquake monitoring. Seismic installations usually avoid sites near railways, and distances of several kilometers between railways and seismic stations are generally recommended (Trnkoczy *et al.*, 2012; Plenkers *et al.*, 2015). A few seismological studies try to utilize train vibrations, for example, as active sources for subsurface imaging (Nakata *et al.*, 2011; Quiros *et al.*, 2016) but do not focus on the characteristics of the train signal itself.

Most available studies on train-induced vibrations take an engineering approach and aim to better understand the generation and short-distance propagation of train-induced vibra-

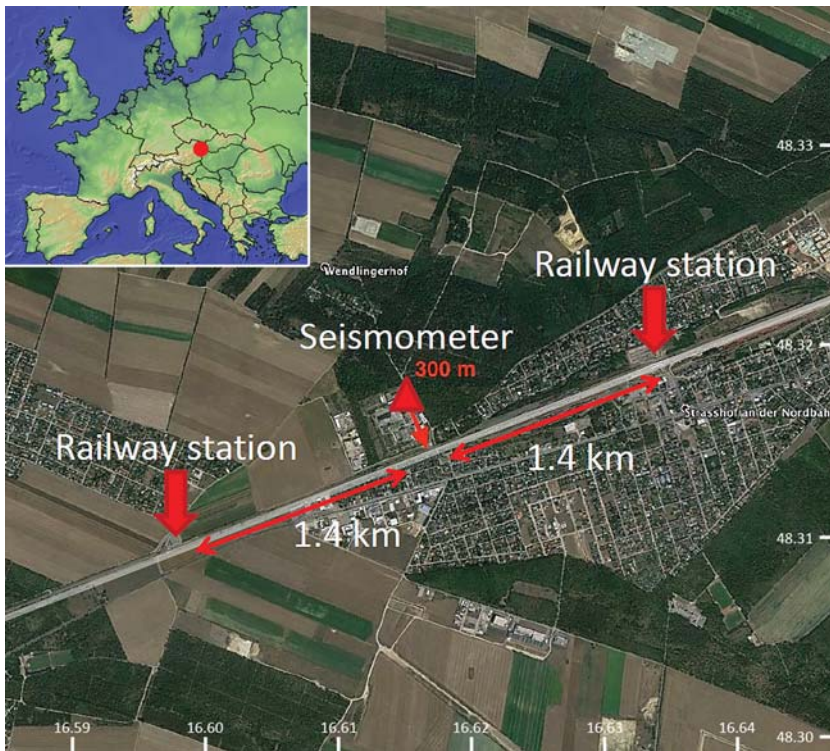
tions, mainly for mitigation and construction purposes (Sheng *et al.*, 2003; Connolly *et al.*, 2015). Studies target the generation of vibrations by moving sources (Ditzel *et al.*, 2001; Wu and Thompson, 2001), the effect of train speed (Kaynia *et al.*, 2000; Degrande and Schillemans, 2001), or ground response and soil characteristics (Yang *et al.*, 2003; Jones, 2010), with a focus on the maximum train-induced ground motion. The majority of those studies rely on numerical simulations and/or short-period or accelerometer recordings obtained directly on the train track or up to few hundred meters away, and almost no studies exist with seismic recordings further away from the track. Chen *et al.* (2004) analyze train vibrations with an array of broadband instruments placed up to 2 km from the track and suggest train vibrations as a potential source for shallow structural imaging. However, their study does not elaborate on the specific characteristics of the train signals themselves. Both Chen *et al.* (2004) and Quiros *et al.* (2016) observe sharp and equidistant peaks in the spectrum of the heavy freight train vibrations but do not attempt to explain them further.

Here we show and analyze various train vibration signals obtained from a set of seismic broadband stations installed in the context of the temporary, large-scale regional seismic network AlpArray (Hetenyi *et al.*, 2016) in central Europe. The geometrical restrictions of this network resulted in a small number of broadband instruments initially deployed in the vicinity of railway lines. On these stations, we observe very characteristic seismic signals associated with different types of trains, all showing pronounced equidistant spectral lines over a wide frequency range. This study analyzes the nature of those signals and discusses if they are generated by a source effect or resemble wave propagation effects in near-surface soil layers. The striking features of train vibrations render them interesting potential sources for seismologists, and identification of train-induced seismic signals by means of their typical characteristics might also facilitate automatic detection of such signals inside data streams.

OBSERVATIONS

Seismic Installation and Methods

As part of the international AlpArray seismic network, we installed 30 broadband seismometers in eastern Austria and western Slovakia (Fuchs *et al.*, 2016) (see Fig. 1 and © Fig. S1,



▲ **Figure 1.** Aerial view of station A002A near Vienna, Austria, where we first discovered the characteristic spectral features of train vibrations discussed in this article. The red dot in the inset denotes the location within Europe. The sensor is offset 300 m from the train track. Railway stations for local commuter trains are in 1.4 km distance from the sensor into both directions along the track.

available in the electronic supplement to this article). Following the strict geometrical constraints of the regular network layout and taking into account other site factors such as accessibility, safety, and power supply led to the temporary deployment of several broadband sensors in the vicinity of railways (some of which were later relocated to improve the noise conditions). We installed all stations discussed in this article in the basement of abandoned or rarely used, such as small huts or farm houses and within 300–1300 m from a railway track. All sensors are RefTek 151 models with a flat instrument response from 50 Hz to 60 s and are equipped with RefTek 130(S) dataloggers, recording continuous data at 100 samples per second (see [Data and Resources](#) for data availability).

To assess how cultural noise affects our seismic stations, we created daily 1-hr-long spectrograms of the vertical component for all 30 stations for a time window at working times (10 a.m. local time) and night times (3 a.m. local time). We computed all spectrograms (window length 5 s with 90% overlap) from raw (not instrument-corrected) ground velocity data which were high-pass-filtered for frequencies above 2 Hz to suppress dominant long-period noise and the microseisms. On all stations that were close to railways, during day times we observed repeating signals of a very prominent shape and characteristics which are associated with passing trains. We describe and discuss these in the following.

Train Signals

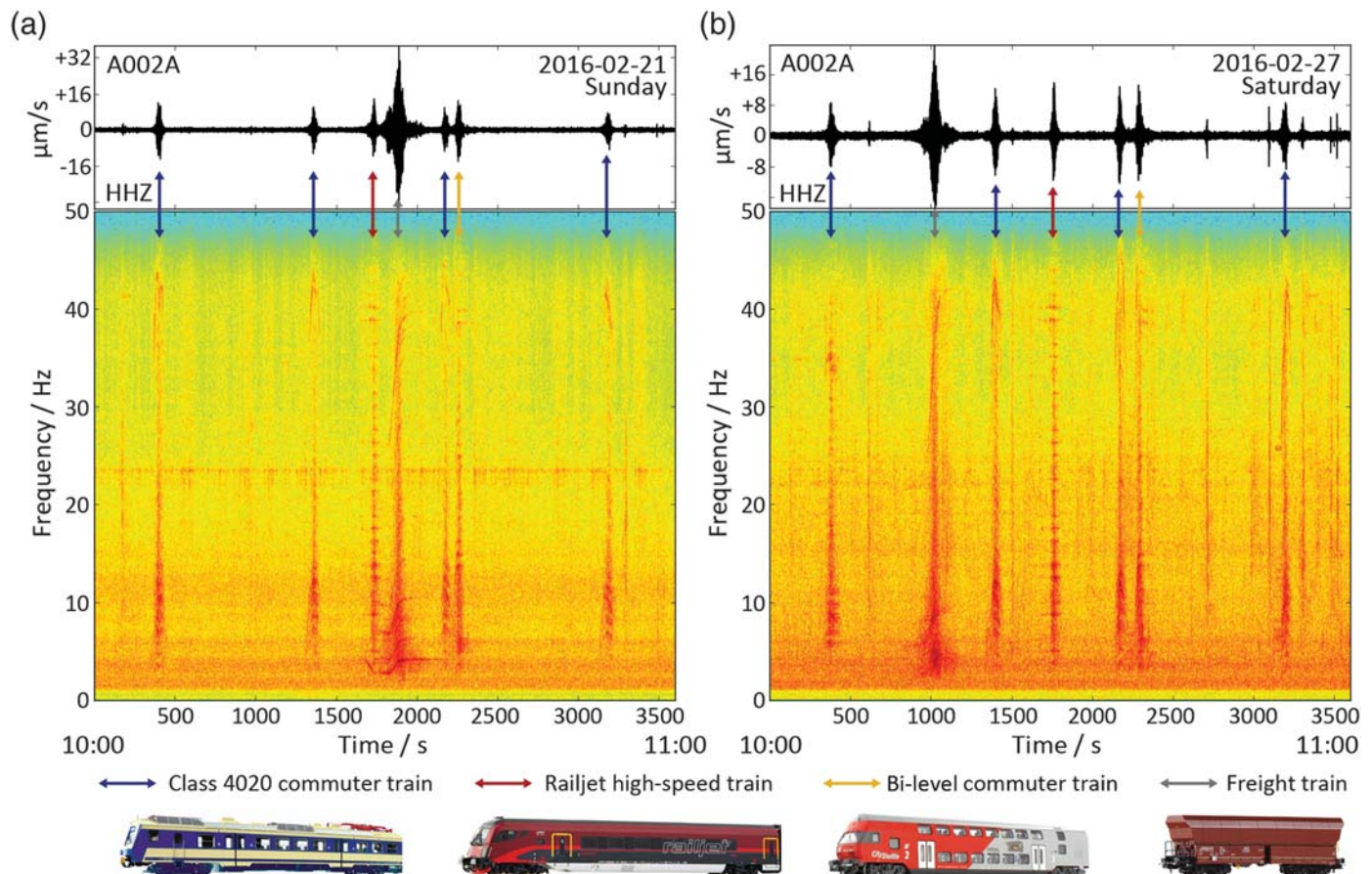
The most well-documented seismic train signals we observe on a site located in the sedimentary Vienna basin, 20 km northeast of Vienna, Austria (see Fig. 1 and © Fig. S1). The station A002A was installed 300 m from the main railway line connecting Vienna to the north, in particular to the Czech Republic. Generally, trains fall in the two categories of passenger trains and freight trains. Passenger trains follow a fixed schedule and are usually serviced by a fixed number of wagons of a fixed type. Freight trains run irregularly and may be operated in all

kind of configurations of numbers or types of wagons. During a site visit, we observed four different types of trains that pass the sensor during the 1-hr time window of the spectrogram. In the following, we introduce these four train types (see Table 1 for structural train details).

1. Local commuter trains pass the sensor four times per hour and stop at train stations at 1.4 km distance to both sides of the sensor. When leaving or approaching a stop, local commuter trains accelerate and decelerate with a rate of $\sim 1 \text{ m/s}^2$, respectively. In between they run at constant speed due to speed limits on the track. At the time of our observations, wagons of type declaration *ÖBB class 4020* were in operation for the local commuter trains.
2. Regional bi-level commuter trains pass the sensor once an hour and stop only at one train station at 4 km distance

Train	Wagons	Length of Wagon (m)	Weight on Axle (t)	Axle Distance (m)	Bogie Distance (m)
Railjet high-speed train	7 + loc.	26.5	17	2.5	19
Class 4020 commuter train	2 × 3	23	10.6	2.3	18.5
Bi-level commuter train	5 + loc.	27	17	2.5	20
Freight train	5–60 + loc.	10–20	10–20	2–9	7–15

For freight trains, the parameters may strongly vary from train to train, and only rough estimates are given (loc. = locomotive).



▲ **Figure 2.** Ground velocity waveforms (upper panels) and spectrograms (lower panels) at station A002A, 300 m from a busy train track. Left and right panels show the same 1-hr time window starting at 10 a.m. local time on a (a) Sunday and (b) Saturday, respectively, when there is little cultural noise other than the train signals. Colored vertical arrows mark the train signals, with the color indicating the type of train (see Table 1 for train details). See Figures 3–5 for a detailed view of individual signals. Spectrograms were calculated with time windows of 5 s and 90% overlap, and the color scale is logarithmic. Note the frequency cutoffs toward 50 Hz (due to the 100-Hz data sampling rate) and below 2 Hz (high-pass filtering to enhance visual signal-to-noise ratio).

ahead of the sensor. There is no stop within 10 km into the other direction. The bi-level trains also accelerate with a rate of $\sim 1 \text{ m/s}^2$ when leaving the train stop until reaching the speed limit. All observed regional bi-level commuter trains were composed of one locomotive and five bi-level wagons.

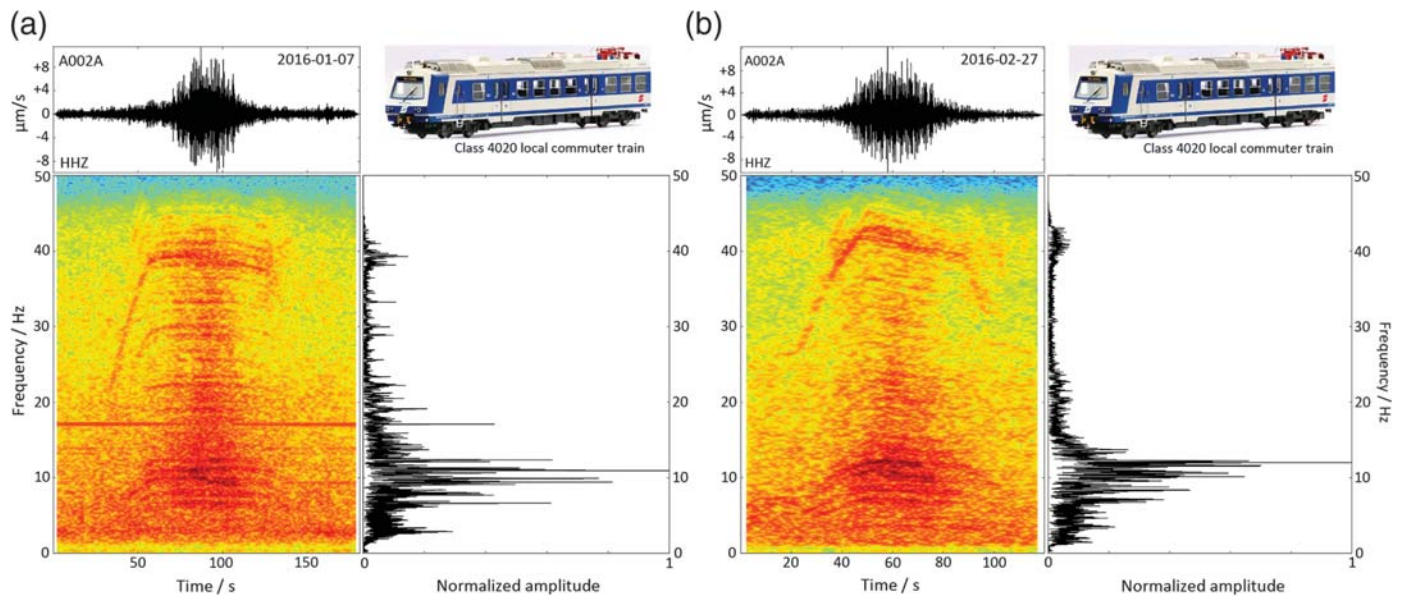
- High-speed trains pass the sensor once an hour with no stops within several kilometers distance and at constant speed. The high-speed trains are of type declaration *Railjet* and consist of one locomotive and seven wagons.
- Freight trains (both loaded and unloaded) pass the station at irregular intervals (not following a fixed schedule).

All of the above trains potentially create individual seismic signals which we analyze separately in the following. The hourly spectrograms obtained on the vertical component for station A002A are dominated by several pronounced peaks that repeat each day and correlate with passing trains (see Fig. 2). The common and most prominent feature of all such peaks is a line spectrum with equally spaced frequencies ranging from < 10 to > 40 Hz. We related visible peaks in the spectro-

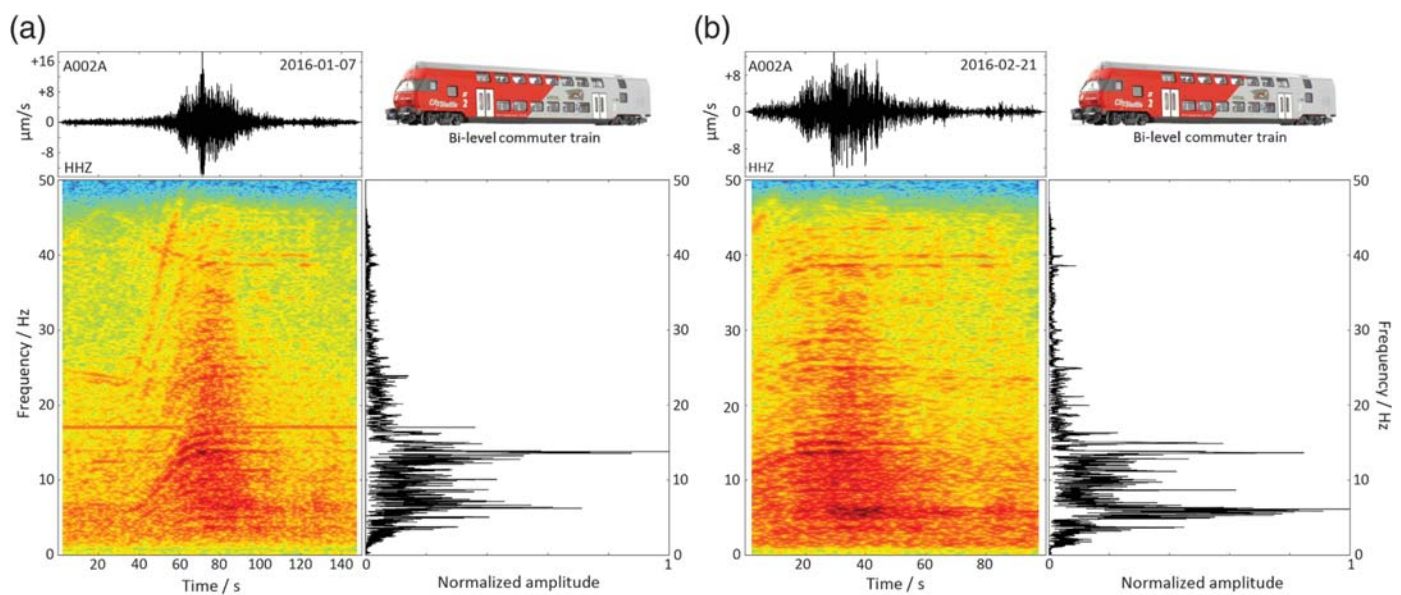
grams to specific trains by referring to train schedules, the site visit, and a web-based real-time train radar application. Commuter, high-speed, and freight trains showed individual characteristic shape in the time-frequency representation, but the regular frequency spacing is visible for all of them.

The onset of local commuter trains seismic recordings (Fig. 3) is characterized by an ~ 20 s long gradual increase of amplitudes and frequencies. The central part of the signal shows almost constant frequencies, the strongest amplitudes, and pronounced spectral lines. Frequencies and amplitudes again decrease gradually within the signal coda. These general features are similar among all local commuter train peaks on any given day. Still, individual trains each have a slightly different shape in the time–frequency representation (see examples in Fig. 3).

The seismic signals of regional bi-level commuter trains (Fig. 4) resemble those of the local commuter trains during the onset phase (increasing frequencies and amplitudes). However, later into the signal we measure constant frequencies with constant line spacing ($\Delta f = 1.27 \text{ Hz}$) that continues into the



▲ **Figure 3.** A002A, Strasshof an der Nordbahn, Austria: Detailed view of two examples of local commuter train signals.



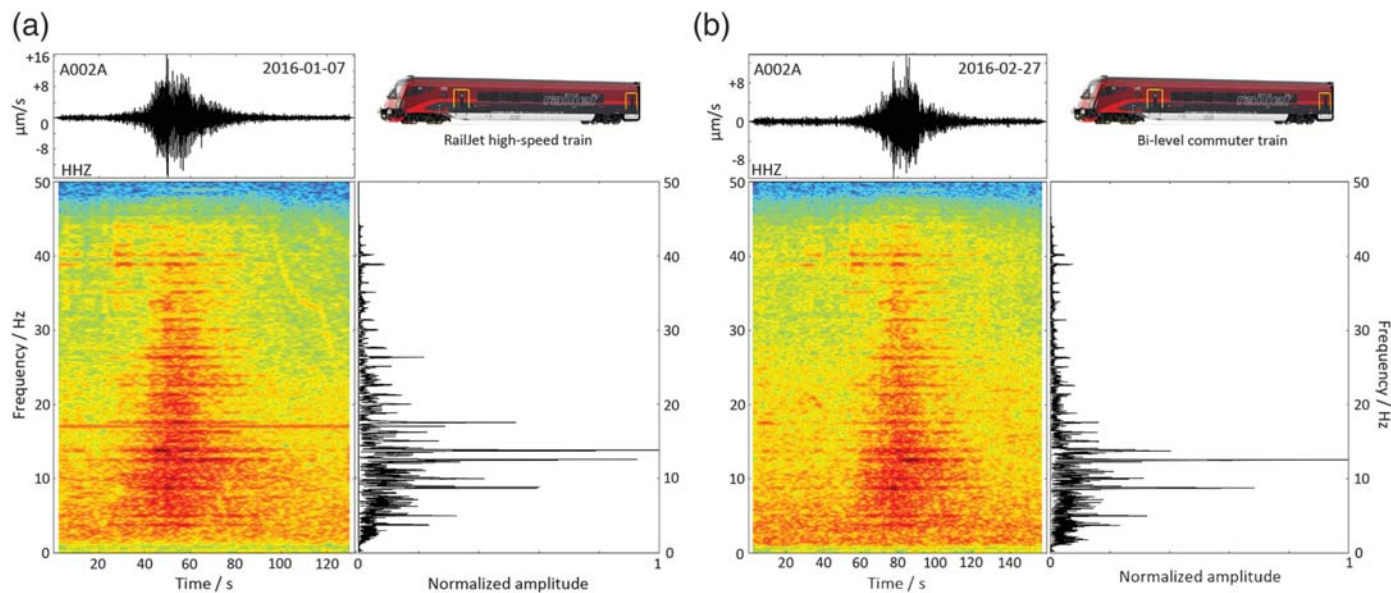
▲ **Figure 4.** A002A, Strasshof an der Nordbahn, Austria: Detailed view of two examples of regional bi-level commuter train signals. The frequency spacing within the flat part is $\Delta f = 1.27$ Hz.

coda, when amplitudes decrease again. Among different days, these main features remain, and despite slightly different onset phases for individual trains the frequencies during the constant part of the signal are almost identical among all days (see e.g., Fig. 4).

High-speed trains induce the most striking vibrations (Fig. 5). The respective spectrograms are dominated by very marked and sharp spectral lines with constant frequency and spacing ($\Delta f = 1.25$ Hz) over the entire signal duration. The vibration spectra of the high-speed trains are remarkably similar (see e.g., Fig. 5) for any individual train on any day.

We relate the seismic signals of the strongest amplitude and the longest duration to freight trains (Fig. 2), due to their heavy weight and large length. The respective records also show equidistant spectral lines, yet the spectrograms of freight trains are more complex in shape.

All train-induced signals show the largest amplitudes around 10 Hz, with a secondary maximum that is sometimes observable around 40 Hz (in particular for local commuter trains, see Fig. 3). Passenger trains induce a maximum vertical ground velocity of $\sim 10\text{--}12$ $\mu\text{m/s}$ at 300 m distance from the track (Fig. 2). This peak ground velocity is only surpassed by



▲ **Figure 5.** A002A, Strasshof an der Nordbahn, Austria: Detailed view of two examples of high-speed train signal. Note the remarkable similarity of the signal on different days (panel a compared to panel b) and the striking regularity of the frequency spacing ($\Delta f = 1.25$ Hz) from below 5 to 40 Hz and above.

heavily loaded freight trains, which induce stronger ground motion.

After the discovery of the train records on station A002A, we searched for similar characteristic signals on all our temporary stations near railways. On all such stations, we discovered seismic signals similar to the ones described above that correlate in time with passing trains (see © Fig. S1). Figure 6 shows selected examples from other installations. Station A024A (Fig. 6c,d) recorded traffic from multiple trains from a 600-m standoff distance to the main east–west railway line in Austria. Hourly vertical-component spectrograms reveal multiple peaks that show the same characteristic sharply delimited spectral lines as the train signals described above for station A002A. However, we did not attempt to relate the seismic recordings to individual trains. Some records resemble the high-speed train signature that we described above (sharply delimited spectral lines of constant line spacing), albeit of narrower frequency spacing $\Delta f = 1.03$ Hz (see Fig. 6c). Yet, many peaks have a more complex shape in the time–frequency representation (Fig. 6d). Figure 6a,b shows additional examples of train records measured on two different sensors, both installed at 1.3 km distance from a railway. Again, multiple spectral lines are visible, yet there are several notable differences: (1) The spectral lines are much wider compared to the observations described above, (2) the spectral lines separate into major maxima with minor maxima in between, and (3) spectral amplitudes are comparable in the entire 10–30 Hz frequency band (Fig. 6a) or decrease constantly toward higher frequencies from a maximum of around 2 Hz (Fig. 6b).

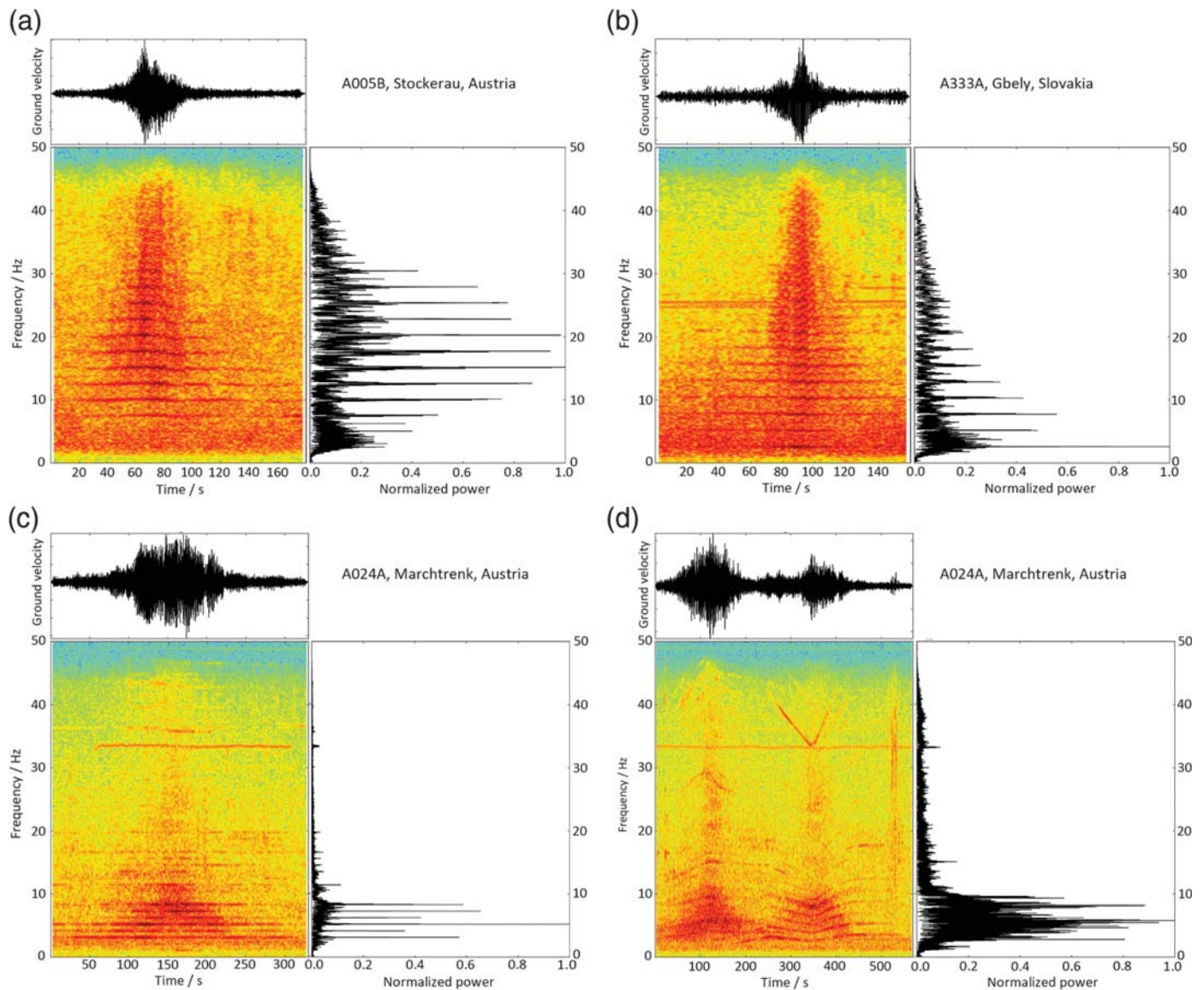
Seismic signals matching the train schedules and similar to the ones described above are also observed on two more stations (A010A, 500 m from a single-track railway and A017A,

360 m from and 175 m above a single track railway) but are not shown in this article. We did not analyze these signals in detail. Still, we conclude that we observe characteristic train signals with regular frequency spacing on all our temporary broadband stations that are or were installed within 1.5 km of a railway.

DISCUSSION

Our seismic data obtained near railway lines show strong signals that are consistent with train-induced vibrations. The dominant features of these signals are pronounced spectral lines with constant spacing over wide frequency intervals that require explanation. Chen *et al.* (2004) also report line spectra with frequency spacing of ~ 1.6 Hz observed for heavy-load freight trains in China and speculate they might be due to resonance features among multiple carriages of the train or reflect predominant frequencies correlated with crustal structure. Degrande and Schillemans (2001) show similar line spectra for high-speed trains but do not comment on it. Quiros *et al.* (2016) show spectrograms of slowly moving freight trains in New Mexico, U.S.A., which strikingly resemble the ones in our study, yet they also do not comment on it.

Our observations show spectra with changing frequencies and frequency spacing (Figs. 3 and 4) and spectra with constant frequencies and spacing throughout the entire signal (Fig. 5). The signal shape in the time–frequency representation is a distinct feature among different types of trains and consistently relates to train speed. For local commuter trains (Fig. 3), the acceleration phase (increasing frequencies when leaving the first stop), the constant speed phase (almost constant frequencies when passing the sensor), and the deceleration phase (decreasing frequencies when approaching the next stop) of



▲ **Figure 6.** Additional examples for characteristic train signals. See © Figure S1 (available in the electronic supplement to this article) for a map of the locations of the seismic stations. (a) Example from A005B, Stockerau, Austria. Sensor is 1.2 km from a two-track railway close to a train stop. Major and minor maxima can be identified with spacings of $\Delta f_1 = 2.54$ Hz and $\Delta f_2 = \Delta f_1/2 = 1.27$ Hz, respectively. We could only identify the source as a local commuter train but the specific type of wagons is unknown to us. (b) Example from A333A, Gbely, Slovakia. Sensor is 1.3 km from a single-track railway. The time window matches a scheduled passenger train, but the specific type of wagons is unknown to us. The frequency spacing is $\Delta f = 2.58$ Hz, with minor maxima exactly centered between the major maxima and a corresponding frequency spacing of $\Delta f = 1.29$ Hz (which is similar to the observations at stations A002A and A005B). The continuous signals around 25 Hz seen in the spectrograms are unlikely to be attributable to train traffic. (c,d) A024A, Marchtrenk, Austria: Two examples recorded at 600 m from a busy two-track railway that is the main east–west connection in Austria. (a,c) Note the sharp and regularly spaced spectral lines, similarly to the lines observed for high-speed trains at station A002A (Fig. 5), but that occupy the lower portion of the frequency axis. The frequency spacing is $\Delta f = 1.03$ Hz. (b,d) Example of more complicated train patterns that likely represent two distinct trains. The regular frequency spacing within individual signals is evident. The continuous signal around 34 Hz is unlikely to be attributable to the trains and instead likely reflects an artificial disturbance, coupling either mechanically or electromagnetically into the seismic acquisition system (Bokelmann and Baisch, 1999).

the trains are visible in each spectrogram. The approximate 20 s duration of the rising flank of the signal corresponds to the time the trains need to accelerate to 70 km/hr with an acceleration of 1 m/s^2 . The slightly different shape of the

two examples in Figure 3 reflects different driving profiles. For regional bi-level commuter trains, only the acceleration part is visible when the trains approach the seismometer (e.g., up to a time of 60 s in Fig. 4a). Later in time into the signal, constant

frequencies reflect constant train speed, whereas trains pass the seismometer and depart. Our data show that the frequency spacing between the spectral lines seems to vary proportionally to train speed (see e.g., Figs. 3 and 4). The spectra of the high-speed trains show constant frequency features throughout the entire signal duration. We attribute this to the remote deployment of A002A from any high-speed train stop. No acceleration or deceleration can be inferred from the spectrograms, and supposedly the speed of high-speed trains is constant within several kilometers distance from the seismometer.

Several spectrograms reveal a continuous spectral line at 16.7 Hz (visible in Figs. 3a, 4a, and 5a), which corresponds to the frequency of the railway power system. We suggest that this feature is not generated by passing trains but is likely coupling electromagnetically into the seismic acquisition system (Bokelmann and Baisch, 1999).

Trains generate ground coupling vibrations through two distinct mechanisms (Connolly *et al.*, 2015): Irregularities on the surface of the wheels or the track (Wu and Thompson, 2001) and the quasi-static load of the ground by the weight of each axle (Kaynia *et al.*, 2000; Yang *et al.*, 2003). Propagation within the shallow subsurface structure additionally shapes the resultant signals recorded at distance (Jones, 2010). In the following, we discuss which effect could create the characteristic line spectra we observe. For simplicity, we focus on the characteristics of the high-speed train signals because they are well documented, reveal the most striking features, and likely represent the simplest case of a train passing at constant speed without any stops nearby.

Track and Wheel Irregularities

We rule out any local stationary sources of vibrations such as bridges or switches (transitions between neighboring, parallel rails) because the observed signal duration (up to 2 min) is much longer than the time needed for the trains to pass any potential stationary irregularity (10 s for a 200-m-long train running at 20 m/s = 72 km/hr). Additionally, no such irregularities were present at the track near station A002A that records some of the most prominent train vibrations. Gaps between segments of the rail are no longer common in modern-day tracks. Small-scale irregularities on the rail surface may create vibrations, but we do not expect those to create constant frequencies (as observed for the high-speed trains) over a distance of several kilometers which the trains travel during the signal duration. In any case, track irregularities should be regarded as repeatedly excited stationary sources.

Wheel irregularities (out-of-roundness) can be a strong source of vibrations. From many of the freight train wagons passing A002A, and from one single high-speed locomotive, a rattling noise originated from the wheels, with frequencies of ~5–7 Hz. This frequency corresponds to the rotation rate of the train wheels (of ~900 mm diameter) for trains running at 50–70 km/hr, a speed which we also confirmed during the site visit. If we consider wheel irregularities as sources of seismic energy, they could be described by delta pulses hitting the rail and repeating at 5–7 Hz. The resulting spectrum would

contain 5–7 Hz as a fundamental frequency with overtones at n times this fundamental frequency. However, most spectra show the strongest amplitudes for frequencies around 10 Hz or higher, and thus we conclude that wheel irregularities may only partly explain the elevated amplitudes around 10 Hz for trains traveling at greater speed. More importantly, the observed frequency spacing of 1–2 Hz is too narrow to reflect overtones of wheel-related fundamental frequencies. We also note that strong wheel irregularities are only expected for old passenger wagons or freight trains which have block brakes but not for present-day passenger trains. Thus, wheel irregularities might only be relevant for a few individual trains but probably do not play a major role in the creation of the line spectra we commonly observe. Additionally, we did not observe any audible rattling for essentially all passenger trains at A002A. We therefore conclude that wheel irregularities do not explain the frequency spacing that we observe in our data. In any case, wheel irregularities would represent moving sources, resulting in measurable Doppler effect.

Static Axle Load

The weight of a train wagon is distributed along the four axles, assembled in pairs of two to the bogies on each end of the wagon. The heavier the load on each individual axle, the bigger the resulting amplitude of ground motion. The quasi-static load of each train axle would result in periodic forcing of the ground, depending on the axle geometry of the respective wagons and the train speed. Table 1 lists the axle geometry of the three train classes studied here in detail. Class 4020 wagons of the local commuter trains have the least axle load (10.6 t) which relates well to the slightly lower amplitudes recorded for all such trains compared to others. High-speed and bi-level wagons have a heavier axle load (17 t) and show up with similar amplitudes in our recordings, only surpassed by freight trains.

The frequencies emitted by the repeating axle load depend on the axle geometry of the train. All types of train wagons passing at A002A have 2.5 m axle distance within one bogie and ~19 m within bogies of the same wagon. Neighboring bogies of two consecutive wagons are ~7.5 m apart. Thus, the respective loading periods are 0.1 s (axle distance), 0.3 s (neighboring bogies of consecutive wagons), and 0.8 s (within the two bogies of one wagon) for a train speed of 85 km/hr. This corresponds to frequencies of 10, 3, and 1.25 Hz, respectively. If we consider one bogie with two axles as the primary source of a periodic load, this mechanism could generate the observed frequency spacing of $\Delta f = 1.25$ Hz. This requires a train speed of 85 km/hr, which is reasonable for the high-speed and bi-level commuter trains at the measuring point of A002A. Thus, we conclude that repeated axle loading of spatially stationary points is the most likely source of the equal spectral line spacing. If we consider segments of the ground below the rails as stationary sources repeatedly excited by the overpassing bogies, the quasi-static axle load mechanism should not involve any Doppler effect.

Propagation Effects

Seismic energy of rail vibrations in the 1–40 Hz frequency range is mostly carried by Rayleigh waves (Jones, 2010; Connolly *et al.*, 2015), which propagate through a shallow and layered soil structure. If the observed regular frequency spacings were due to propagation effects, train signals might potentially facilitate detailed studies of shallow wave propagation, soil layering, and attenuation. However, we conclude that shallow soil layers cannot explain the observed regular frequency spacing for the following reasons.

The observed line spacing is too regular and extends over a frequency range too wide to reflect higher modes of Rayleigh-wave propagation. Jones (2010) calculates Rayleigh-wave dispersion diagrams specifically for the setting of railway tracks on top of a layered structure, but the resulting mode structure cannot explain the regular frequency spacing. Furthermore, individual peaks in the spectra are too narrow to be caused by reflection resonances within soil layers (e.g., peaks in commonly observed horizontal-to-vertical spectra are usually several hertz wide). To create such sharp resonance, peaks would require unrealistic seismic impedance contrasts between shallow layers. Additionally, different train types show different frequencies, and most importantly the generated frequencies clearly depend on the train speed. If the spectral lines were caused by a propagation effect due to ground features, the effect should be similar for all trains and should not vary smoothly with train speed. Only certain frequencies could resonate within soil layers and thus a continuous transition from lower to higher frequencies with increasing line spacing should not be possible, but is clearly observed.

All of the train-related mechanisms above would generate frequencies proportional to the train speed, but only the quasi-static axle load in combination with the bogie geometries seems capable of creating the observed narrow frequency spacing of 1–2 Hz. We performed two additional tests to narrow down the possible source mechanism.

Cepstrum Analysis

To identify potentially repeating sources in the train waveforms that may create the observed frequency spacing and relate to one of the source mechanisms above, we performed a cepstrum analysis. The cepstrum is an analysis tool that reveals repeating patterns in continuous waveforms such as echoes (Oppenheim and Schaffer, 2004). A cepstrum is calculated as the inverse Fourier transform of the logarithmic absolute value of the original spectrum. Peaks in the cepstrum correspond to periods at which certain patterns in the waveforms repeat. Figure 7 shows the cepstrum calculated for a high-speed train in comparison with the time-domain waveform and the common frequency domain spectrum. The cepstrum main peak indicates a waveform pattern repeating each 0.8 s; we visually confirmed these repeated patterns within the waveforms. This corresponds exactly to the frequency spacing $\Delta f = 1/0.8 \text{ s} = 1.25 \text{ Hz}$ which is observed in the spectrum. Similarly, when analyzing, for example, the flat part of the bi-level commuter trains, a cepstrum peak is found which cor-

responds to the inverse frequency spacing. Hence, the cepstrum analysis reveals that our records of trains running at constant speed are dominated by a signal pattern that repeats each 0.8 s. This matches well the expected forcing period for a bogie distance of 19 m (as is the case for both the high-speed train and the bi-level commuter train) and a train speed of 85 km/hr and may thus explain the observed line spectrum with a frequency spacing of $\Delta f = 1.25 \text{ Hz}$. The cepstrum also contains a peak at 0.3 s, which potentially relates to the distance between the two neighboring bogies of consecutive wagons (7.5 m) and a speed of 85 km/hr. We cannot identify any peaks at shorter periods that could relate to individual axles (2.5 m apart) or the railway ties (0.6 m apart), using our cepstral analysis.

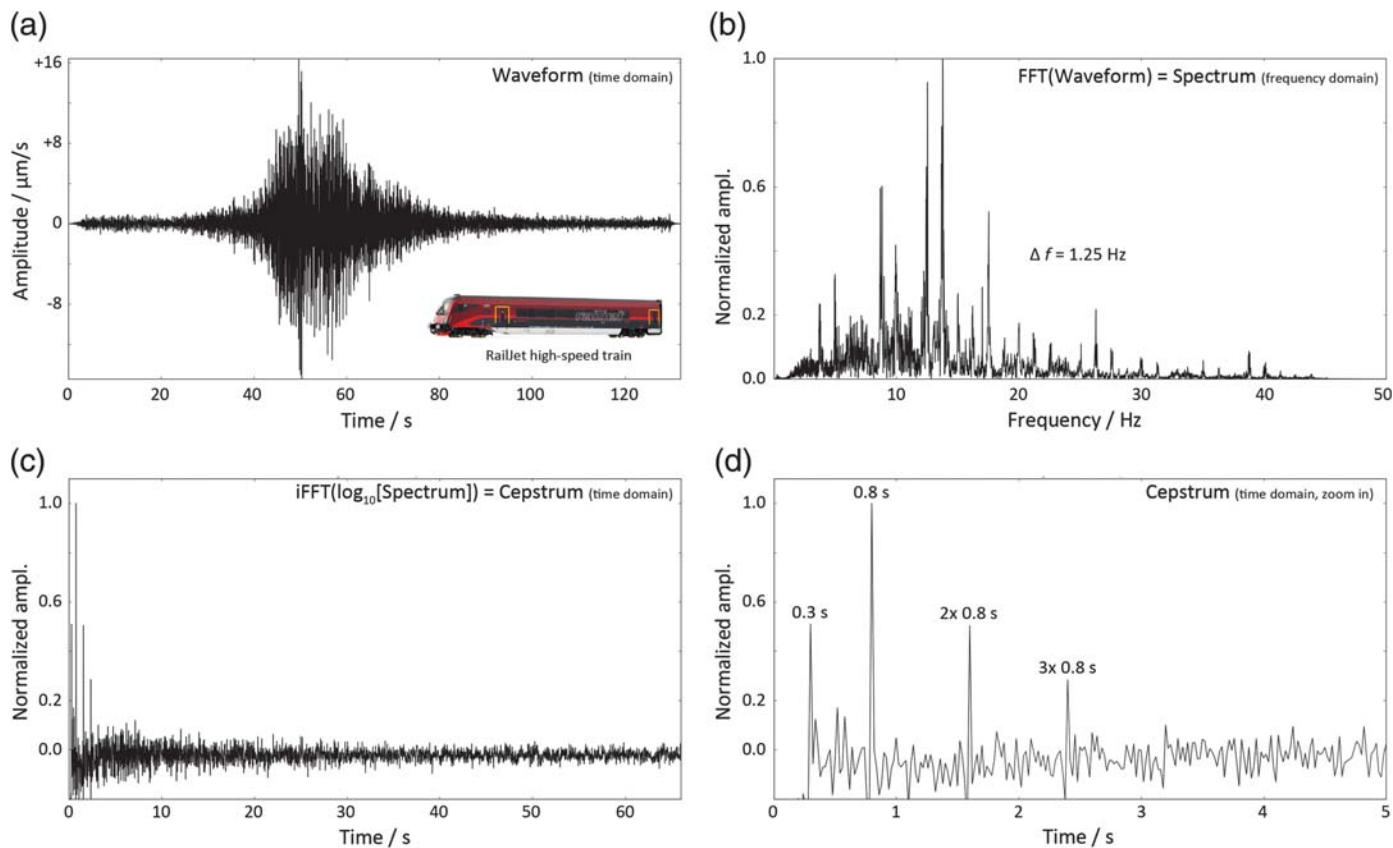
Doppler Effect

Irregularities on the wheels should be considered as repeating and moving sources, whereas both irregularities on the track and the static axle load are stationary repeating sources. For any moving source, we would expect a Doppler effect visible in the spectrogram or by comparison of spectra of the approaching and departing train. Previous studies, for example, Quiros *et al.* (2016) claim to observe Doppler effect in spectrograms, judged from higher frequency content in the approaching part of signal as compared to the departing part. Chen *et al.* (2004) observe a Doppler effect seen by comparison of spectra of the approaching and departing train.

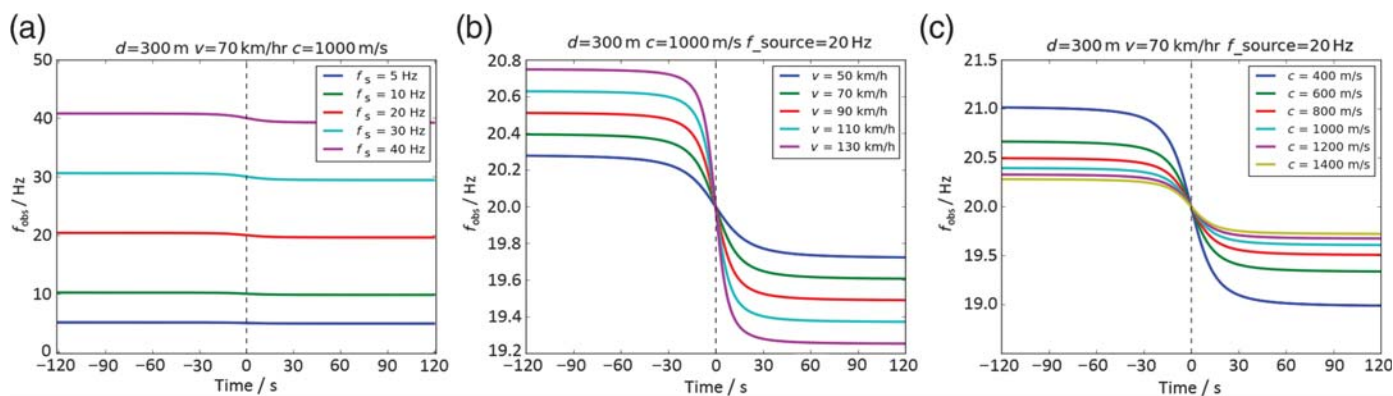
To assess if the source of the vibrations is stationary or moving, we analyzed potential Doppler effects for the geometry at station A002A. In most of the train spectrograms in this work, there is no clear indication of a Doppler effect (see e.g., Figs. 3–5). In particular, the signals for the high-speed trains show constant frequencies over the entire signal duration (Fig. 5). Bi-level commuter trains which pass the station at supposedly constant speed do also not show any indication of a Doppler effect (Fig. 4). For other trains such as the local commuter train class 4020, the spectrogram is dominated by effects of varying train speed rather than a potential Doppler effect (Fig. 3).

To check if a Doppler effect should leave a notable signature in our spectrograms, we calculated the expected frequency shift for a passing source for various parameters (see Fig. 8). Frequency shifts of up to 2 Hz between an approaching and departing train would be expected for a station 300 m from the track (such as A002A), depending predominantly on train speed and the seismic wave propagation velocity. However, Figure 8a demonstrates that such a frequency shift would be difficult to observe in spectrograms scaled from 0 to 50 Hz. Thus, we compared the spectra of approaching and departing trains separately but could not identify any clear frequency shifts. Additionally, the main cepstrum peaks of the approaching and departing part of the signal are identical.

Only on one seismic station, some records resemble the theoretically expected frequency shifts in the central part of the spectrogram (⊕ Fig. S2). However, the station is comparably far from the track (1.2 km), which reduces any Doppler effect, and at this track we expect only moderate train speeds.



▲ **Figure 7.** Cepstrum analysis for a high-speed train (Fig. 5). (a) Waveform in units of velocity. (b) Spectrum of the waveform shown in (a). (c) Cepstrum of the waveform shown in (a). (d) Magnified profile of the main peaks in the cepstrum. The highest peak in the cepstrum (0.8 s) corresponds to a frequency spacing of $\Delta f = 1/0.8 \text{ s} = 1.25 \text{ Hz}$. The peaks at longer periods are higher orders of the main peak. A patch of signal repeating each 0.8 s is also visible in the waveforms when the horizontal axis is dilated (zoomed in).



▲ **Figure 8.** Calculated Doppler effect with variable parameters. The distance of the seismometer to the track is fixed to 300 m. (a) Variable source frequencies, train speed $v = 70 \text{ km/hr}$, and propagation velocity $c = 1 \text{ km/s}$; (b) variable train speed, source frequency $f = 20 \text{ Hz}$, and propagation velocity $c = 1 \text{ km/s}$; and (c) variable propagation velocity, train speed $v = 70 \text{ km/hr}$, and source frequency $f = 20 \text{ Hz}$. Frequency shifts of up to 2 Hz between an approaching and departing train would be expected, depending on train speed and seismic wave-propagation velocity. Note that given the frequency scale of the spectrograms in this work (see panel a, 0–50 Hz), clear Doppler effects may only be directly observed for slow seismic velocities and higher source frequencies because Doppler effect is proportional to the source frequency.

Thus, very low-seismic velocities would be required to create a Doppler effect.

CONCLUSIONS AND OUTLOOK

We analyzed in detail the seismic vibrations generated by trains and measured at distance from the track with high sensitivity broadband sensors. We recorded seismic signals within 1.5 km of railways for which frequency characteristics appear quantified by train passage loading. All train signals share the main feature of sharp equidistant spectral lines in the entire 2–40 Hz frequency range. We could not analyze higher frequencies because of Nyquist frequency limitations. For one site located 300 m from a busy track, we studied the train records in detail and were able to relate them to individual trains. The frequency spacing is 1–2 Hz and relates to train speed. We further identify acceleration, constant speed, and deceleration phases using spectrograms of the individual trains, which we could then attribute to specific train driving profiles.

Based on the missing Doppler effect and the cepstrum analysis of repeating signal patches, we conclude that the observed spectral lines are likely no overtone phenomenon as, for example, observed for seismic helicopter noise (Eibl *et al.*, 2015). Rather, we suggest that the dominant mechanism behind the 1–2 Hz line spacing is a repeated forcing of the ground by quasi-static axle load which primarily acts through the bogies of each train wagon. For a reasonable train speed of 85 km/hr at the measuring site and a typical bogie separation of 19 m, the loading period of 0.8 s matches well the inverse frequency spacing of 1.25 Hz for high-speed trains that pass the site at constant speed.

We note, however, that the overall train signal might be shaped by more factors than just the quasi-static axle load. Especially, the amplitude distribution in the frequency domain requires additional mechanisms, and likely a combination of many factors is responsible for the cumulative signal characteristics. The complex, yet puzzling features of the train records still require more explanation, and we plan to perform targeted field experiments with portable short-period arrays in the future.

The striking feature of equidistant spectral lines within the train vibrations was already documented in earlier studies (Degrande and Schillemans, 2001; Chen *et al.*, 2004; Quiros *et al.*, 2016), yet was never properly commented on or analyzed. Based on our documentation, seismic train signals could be automatically identified and removed from data streams in case they are considered unwanted noise. However, we also highlight the potential use of such signals as training material for students, especially when made audible (Kilb *et al.*, 2012). The particular characteristics of the train vibrations render them quite outstanding among the seismic sources which seismologists usually deal with. Nakata *et al.* (2011) and Quiros *et al.* (2016) suggest to use train vibrations as a source for structural imaging, even without making use of the distinctive signal characteristics. Because some of the train vibrations, for example, those of high-speed trains observed in this study, almost

represent a source which could be called a seismic frequency comb, we speculate that such signals might be particularly useful, for example, frequency-dependent attenuation measurements, near-surface wave propagation studies, or certain applications such as targeted subsurface imaging.

DATA AND RESOURCES

This study is based on data from the [AlpArray Seismic Network \(2015\)](#) which at the time of publication was not publicly available (www.alparray.ethz.ch, last accessed October 2017) for more details on data access. Visit http://data.datacite.org/10.12686/alparray/z3_2015 (last accessed October 2017) for more information on the AlpArray seismic network. All data processing and plotting were done using the ObsPy toolbox (Krischer *et al.*, 2015). ✉

ACKNOWLEDGMENTS

This work was funded by the Austrian Science Fund FWF Project Number P26391. The authors thank Peter Steinhauser for discussions and helpful information. The authors acknowledge help during field work by Maria-Theresia Apoloner, Gidera Gröschl, Johann Huber, Petr Kolinsky, Ehsan Qorbani, Eric Löberich, Sven Schippkus, and Felix Schneider. Please visit www.alparray.ethz.ch for a complete list of people contributing to the AlpArray seismic network.

REFERENCES

- AlpArray Seismic Network (2015): *AlpArray Seismic Network (AASN) Temporary Component*, AlpArray Working Group, Datacite link: http://data.datacite.org/10.12686/alparray/z3_2015; Project webpage: <http://www.alparray.ethz.ch/home> (last accessed October 2017).
- Bokelmann, G., and S. Baisch (1999). Nature of narrow-band signals at 2.083 Hz, *Bull. Seismol. Soc. Am.* **89**, 156–164.
- Chen, Q., L. Li, G. Li, L. Chen, W. Peng, Y. Tang, Y. Chen, and F. Wang (2004). Seismic features of vibration induced by train, *Acta Seismol. Sinica* **17**, 715–724, doi: [10.1007/s11589-004-0011-7](https://doi.org/10.1007/s11589-004-0011-7).
- Connolly, D., G. Kouroussis, O. Laghrouche, C. Ho, and M. Forde (2015). Benchmarking railway vibrations—Track, vehicle, ground and building effects, *Constr. Build. Mater.* **92**, 64–81, doi: [10.1016/j.conbuildmat.2014.07.042](https://doi.org/10.1016/j.conbuildmat.2014.07.042).
- Degrande, G., and L. Schillemans (2001). Free field vibrations during the passage of a Thalys high-speed train at variable speed, *J. Sound Vib.* **247**, 131–144, doi: [10.1006/jsvi.2001.3718](https://doi.org/10.1006/jsvi.2001.3718).
- Ditzel, A., G. C. Herman, and G. G. Drijkoningen (2001). Seismograms of moving trains: Comparison of theory and measurements, *J. Sound Vib.* **248**, 635–652, doi: [10.1006/jsvi.2001.3807](https://doi.org/10.1006/jsvi.2001.3807).
- Eibl, E. P., I. Lokmer, C. J. Bean, E. Akerlie, and K. S. Vogfjörd (2015). Helicopter vs. volcanic tremor: Characteristic features of seismic harmonic tremor on volcanoes, *J. Volcanol. Geoth. Res.* **304**, 108–117, doi: [10.1016/j.jvolgeores.2015.08.002](https://doi.org/10.1016/j.jvolgeores.2015.08.002).
- Fuchs, F., P. Kolinsky, G. Gröschl, G. Bokelmann, and the AlpArray Working Group (2016). AlpArray in Austria and Slovakia: Technical realization, site description and noise characterization, *Adv. Geosci.* **43**, 1–13, doi: [10.5194/adgeo-43-1-2016](https://doi.org/10.5194/adgeo-43-1-2016).
- Hetenyi, G., I. Molinari, J. Clinton, and E. Kissling (2016). The AlpArray Seismic Network: Current status and next steps, *Geophys. Res. Abstr.* **18**, EGU2016-11744–1.

- Jones, C. (2010). Low frequency ground vibration, in *Railway Noise and Vibration*, D. Thompson (Editor), Elsevier Ltd., 399–433, doi: [10.1016/B978-0-08-045147-3.00012-8](https://doi.org/10.1016/B978-0-08-045147-3.00012-8).
- Kaynia, A. M., C. Madshus, and P. Zackrisson (2000). Ground vibration from high-speed trains: Prediction and countermeasure, *J. Geotech. Geoenviron. Eng.* **126**, 531–537, doi: [10.1061/\(ASCE\)1090-0241\(2000\)126:6\(531\)](https://doi.org/10.1061/(ASCE)1090-0241(2000)126:6(531)).
- Kilb, D., Z. Peng, D. Simpson, A. Michael, M. Fisher, and D. Rohrlick (2012). Listen, watch, learn: SeisSound video products, *Seismol. Res. Lett.* **83**, 281–286, doi: [10.1785/gssrl.83.2.281](https://doi.org/10.1785/gssrl.83.2.281).
- Krischer, L., T. Megies, R. Barsch, M. Beyreuther, T. Lecocq, C. Caudron, and J. Wassermann (2015). ObsPy: A bridge for seismology into the scientific Python ecosystem, *Comput. Sci. Discov.* **8**, 014003, doi: [10.1088/1749-4699/8/1/014003](https://doi.org/10.1088/1749-4699/8/1/014003).
- Nakata, N., R. Snieder, T. Tsuji, K. Larner, and T. Matsuoka (2011). Shear wave imaging from traffic noise using seismic interferometry by cross-coherence, *Geophysics* **76**, SA97–SA106, doi: [10.1190/geo2010-0188.1](https://doi.org/10.1190/geo2010-0188.1).
- Oppenheim, A. V., and R. W. Schaffer (2004). From frequency to que-
frequency: A history of the cepstrum, *IEEE Signal Process. Mag.* **21**, 95–106, doi: [10.1109/MSP.2004.1328092](https://doi.org/10.1109/MSP.2004.1328092).
- Plenkens, K., S. Husen, and T. Kraft (2015). A multi-step assessment
scheme for seismic network site selection in densely populated areas,
J. Seismol. **19**, 861–879, doi: [10.1007/s10950-015-9500-5](https://doi.org/10.1007/s10950-015-9500-5).
- Quiros, D. A., L. D. Brown, and D. Kim (2016). Seismic interferometry
of railroad induced ground motions: Body and surface wave
imaging, *Geophys. J. Int.* **205**, 301–313, doi: [10.1093/gji/ggw033](https://doi.org/10.1093/gji/ggw033).
- Sheng, X., C. J. C. Jones, and D. J. Thompson (2003). A comparison of a
theoretical model for quasi-statically and dynamically induced
environmental vibration from trains with measurements, *J. Sound
Vib.* **267**, 621–635, doi: [10.1016/s0022-460x\(03\)00728-4](https://doi.org/10.1016/s0022-460x(03)00728-4).
- Trnkoczy, A., P. Bormann, W. Hanka, L. G. Holcomb, R. L. Nigbor, M.
Shinohara, H. Shiobara, and K. Suyehiro (2012). Site selection,
preparation and installation of seismic stations, in *New Manual
of Seismological Observatory Practice 2 (NMSOP-2)*, P. Bormann
(Editor), Deutsches GeoForschungsZentrum GFZ, Potsdam,
Germany, 1–139, doi: [10.2312/GFZ.NMSOP-2_ch7](https://doi.org/10.2312/GFZ.NMSOP-2_ch7).
- Wu, T. X., and D. J. Thompson (2001). Vibration analysis of railway
track with multiple wheels on the rail, *J. Sound Vib.* **239**, 69–
97, doi: [10.1006/jsvi.2000.3157](https://doi.org/10.1006/jsvi.2000.3157).
- Yang, Y., H. Hung, and D. Chang (2003). Train-induced wave propaga-
tion in layered soils using finite/infinite element simulation, *Soil
Dynam. Earthq. Eng.* **23**, 263–278, doi: [10.1016/s0267-7261\(03\)00003-4](https://doi.org/10.1016/s0267-7261(03)00003-4).

Florian Fuchs
Götz Bokelmann
Department of Meteorology and Geophysics
University of Vienna
Althanstraße 14, UZA 2
1090 Vienna, Austria
florian.fuchs@univie.ac.at

Published Online 8 November 2017